Optical investigation of the *DX* centers in GaAs under hydrostatic pressure

Jan Zeman
High Magnetic Field Laboratory, Max-Planck-Institut für Festkörperforschung and Centre National de la Recherche Scientifique, Boîte Postale 166, 38042 Grenoble Cedex 9, France and Institute of Physics, Academy of Sciences of the Czech Republic, Cukrovarnická 10, 16200 Praha 6, Czech Republic

Michel Zigone and Gérard Martinez
High Magnetic Field Laboratory, Max-Planck-Institut für Festkörperforschung and Centre National de la Recherche Scientifique, Boîte Postale 166, 38042 Grenoble Cedex 9, France
(Received 11 October 1994)

Raman-scattering experiments performed on *n*-type GaAs samples, doped with Te, Si, and S impurities, as a function of hydrostatic pressure in the indirect-gap range 4–9 GPa, reveal the bistable character of the related impurity level under optical illumination. A numerical simulation of our results shows that the negative-*U* model of Chadi and Chang is valid for reproducing the experimental data at low pressure. However, at very high pressures beyond 5–6 GPa, a positive-*U* description involving a small lattice relaxation is necessary to reproduce results for Te- and Si-doped samples. This demonstrates that the *DX* defect evolves under pressure, and that a transition from negative to positive *U* can occur at about 5–6 GPa.

I. INTRODUCTION

The *DX* center in $Al_xGa_{1-x}As$ alloys and *n*-doped GaAs has been intensively investigated these last 15 years. However, a clear understanding of this defect has not yet been achieved. This understanding is very important because *DX* centers appear inevitably in many *n*-type III-V compounds semiconductors, and limit the performance of optoelectronic devices.

The *DX* center is known to be induced by the presence of *n*-type impurities in $Ga_xAl_{1-x}As$ alloys when the Al concentration exceeds 22%, or in GaAs when a hydrostatic pressure above 2.5 GPa is applied.[1–4] It is characterized by a deep center behavior and a persistent photoconductivity (PPC), though the latter is not a specific property of the center. The discovery of the *DX* center in *n*-type GaAs under hydrostatic pressure was an important step in studying this defect.[5–8] Indeed, it has been considered as direct proof of the relation between the *DX* center and the substitutional impurity which presents at least two different type of energy states: deep and shallowlike. Thus the stability of the deep state for $x > 0.25$ in $Al_xGa_{1-x}As$ and for pressures beyond 2.5 GPa in *n*-type GaAs has the same origin and is related to band-structure effects, a consequence of the similarity of hydrostatic pressure and alloying[5–7] on the band structure. The advantage of the hydrostatic pressure tool is to modify the band structure of the material on a single sample, in a reversible way, without inducing extra perturbation.

Various techniques have been used in experiments under hydrostatic pressure: electrical or optical measurements under pressure such as the Hall effect,[6–10] Shubnikov–de Haas[4,7] oscillations, deep-level transient spectroscopy (DLTS),[8,11–14] and photoluminescence.[4,15–17] They have revealed the existence of *DX* centers associated with different impurities such as Si, Sn, S, Te, and Se. However, the energy position of the *DX* level in GaAs as a function of pressure is not yet well determined. It is now accepted that the deep *DX* level enters the forbidden gap of GaAs at around 2.5 GPa, but in the indirect-gap regime (i.e., for pressures beyond 4 GPa), the behavior of the center under pressure has been investigated very little.[18–20]

Recently, we performed Raman-scattering experiments on *n*-type GaAs as a function of hydrostatic pressure, which have revealed the existence, at low temperature and beyond some critical value of the pressure corresponding to the indirect-gap regime, of bound phonons associated with electrons trapped at an effective-mass-like level.[19,20] At higher temperatures, this level is depopulated in favor of a deep state which has many of the characteristics of the *DX* center. These results indicate a shallow-deep bistable character of *n*-type impurities in GaAs under high pressure. This bistability has already been studied by various techniques such as the Hall effect,[21,22] infrared absorption,[23] electron paramagnetic resonance (EPR),[24,25] and DLTS (Ref. 26) in GaAs and $Ga_{1-x}Al_xAs$, and appears to be a general property in III-V semiconductors.[27,28]

It is generally accepted that the *DX* center is a substitutional isolated donor which undergoes a shallow-to-deep donor transition under the above conditions of alloying or application of hydrostatic pressure. The description of the defect, proposed by Chadi and Chang,[29] is based upon the concept of a negative-*U* defect center, i.e., a negatively charged donor DX^-, highly localized and exhibiting a large lattice relaxation (LLR) effect. More recently, Zhang and Chadi[30] simulated the effect of pressure (or Al alloying) on that DX^- level in GaAs (or $Al_xGa_{1-x}As$ alloys), and have shown that this level enters the gap of GaAs at around 2 GPa (or for an

aluminum concentration of about 20% in $Ga_{1-x}Al_xAs$), in fair agreement with experimental results. The Chadi and Chang model appears to explain most of the basic properties of the *DX* center, at least in the direct-gap regime,[22,31,32] but its validity remains to be confirmed at very high pressures.

Among other models, a simpler description has been given by Dmochowski *et al.*,[23] who proposed that the *DX* center has only two charge states, namely D^0 and D^+, with two different configurations for the D^0 state corresponding to one deep level and one shallow level. This model corresponds to a positive-*U* situation. With this model Dmochowski *et al.* were also able to reproduce various experiments such as the Hall effect and infrared absorption.[23] Another calculation based on first principles has also been performed on these defects in GaAs and $Ga_{1-x}Al_xAs$, and has lead to a positive-*U* picture associated with a small lattice reaction (SLR).[33]

The purpose of this paper is to present an experimental study of both the metastable hydrogenlike state and the deep level associated with the *DX* center in GaAs doped with different *n*-type impurity species (S, Te, and Si) under high hydrostatic pressure in the range 4–9 GPa (indirect-gap regime). Whereas, for such high pressures, transport techniques are very difficult to perform under hydrostatic conditions, optical techniques, such as Raman experiments using diamond-anvil cells (DAC), allow us to work in quasihydrostatic conditions (better than 1%) up to 12 GPa, and can be used to probe the free-carrier concentration.

From these data one can deduce the properties of the energy levels of the center as a function of the pressure for different donor species. The Raman spectrum of *n*-doped GaAs can give information about the concentration of free electrons because of the interaction between the longitudinal-optic (LO) mode and the collective excitations of these electrons. The method is described in more detail in Sec II.

The present paper is divided into six sections: Sec. II contains a description of the experiments under hydrostatic pressure, which are analyzed in Sec. III. Section IV presents the rate equations which have been used for a numerical simulation of our experimental results, in the framework of the theoretical descriptions given by Dmochowski *et al.*[23] and Chadi and Chang.[29] In Sec. V, a comparison with experimental data is outlined. As a result, it is proposed that there are two different behaviors of the center depending on the pressure range: if the negative-*U* model is consistent with data at lower pressures, only the two-charge state model of Dmochowski *et al.* (positive *U*) can reproduce the experimental data at higher pressures for Si and Te impurities. Conclusions are drawn in Sec. VI.

II. EXPERIMENT

Our results have been obtained on three different *n*-type GaAs samples doped during growth (by Bridgman's technique) with tellurium (sample *A*, $n=2\times10^{18}$ cm^{-3}), silicon (sample *B*, $n=2\times10^{18}$ cm^{-3}), or sulfur (sample *C*, $n=3\times10^{18}$ cm^{-3}). For the Te- and S-doped samples the compensation rate is less than 10%. In the range of donor concentrations which have been explored, we are well below the metal-insulator transition for the indirect-gap regime. Another sample (sample *D*) made of unintentionally doped GaAs ($n<10^{16}$ cm^{-3}), was also used as a reference for measuring the transverse- and longitudinal-optic modes (TO) and (LO) modes at various pressure and temperature conditions.

Raman-scattering experiments have been performed as a function of hydrostatic pressure on these samples using the DAC technique. A 4:1 mixture of methanol-ethanol was chosen as the pressure-transmitting medium. The value of the pressure was measured using the calibrated shift of the ruby luminescence line, by including tiny ruby pieces in the pressure chamber along with the sample. The pressure determination was accurate to ±0.1 GPa. All pressure changes were made at room temperature. No pressure dependence of the phonon linewidths has been detected, indicating a negligible amount of nonhydrostatic stress (<0.1 GPa). In order to investigate the temperature dependence, the DAC was inserted in a helium flow cryostat, and the temperature was measured using a carbon and platinum resistor glued to the heat sink. The actual temperature of the sample has been checked systematically by recording that of the ruby chip located close to it. These experiments have been performed with the use of a triple Raman spectrograph DILOR operating in the high dispersion mode with multichannel detection. The resolution of this apparatus reaches 0.2 cm^{-1}. The red line 647.1 nm of a krypton laser has been used for excitation.

A typical Raman spectrum of pure GaAs consists of LO and TO lines. Their position depends on the pressure, but the splitting is virtually independent of the pressure, temperature, or laser intensity. In highly *n*-doped samples, a coupling appears at high temperature between the LO mode and plasmons,[34] giving rise to so-called ω_+ and ω_- modes. Under such conditions, one usually measures the TO peak and a line corresponding to the ω_+ mode. The position of this peak depends on pressure and also on the free-electron concentration n_c and consequently on the temperature. The splitting $\Delta\omega=\omega_+-\omega_{TO}$ reflects this effect. The free-electron concentration influences also the half-width of the ω_+ peak, which broadens when temperature increases. In a certain temperature range (250–300 K) and for certain pressures, n_c is sensitive to the intensity of the incident laser beam due to the bistability of the *DX* center. In those conditions the position of the ω_+ mode is sensitive to the laser power. All these effects have been demonstrated in our previous work.[19,20] Besides TO and ω_+ peaks, we observe (in doped samples and at low temperatures) small Raman structures at a lower energy than the ω_+ mode which are due to bound phonons. These bound phonons have already been investigated elsewhere.[19]

The experimental procedure consists of recording, at a given value of the pressure and at different temperatures, Raman spectra for two different laser power intensities I_0 and $I_0/20$. The splitting $\Delta\omega$ between the TO- and the LO-plasmon collective mode is followed for the two different power intensities as a function of temperature,

and the results are presented in Figs. 1, 2, and 3 for different impurity species and for different values of pressure. Two regimes are clearly apparent: at low temperature $\Delta\omega$ is not sensitive to the laser power intensity. It increases in a way which reproduces the impurity ionization from the effective-mass-like level of the impurity. Above a critical temperature, around 200 K for all impurities, the spectra become laser power dependent but in a way which varies with the species. Thus different behaviors can be observed in Figs. 1, 2, and 3 in this high-temperature regime, which correspond to different regimes of thermal ionization that we are going to analyze.

III. ANALYSIS OF THE EXPERIMENTAL RESULTS

The free-carrier concentration n_c can be determined through the plasmon frequency $\omega_P^2=(4\pi n_c e^2)/(\varepsilon_\infty m^*)$, which in turn is deduced from our measurements of $\Delta\omega$ using the relation[34] $\omega_P^2=\omega_+^2[(\omega_{LO}^2-\omega_+^2)/(\omega_{TO}^2-\omega_+^2)]$, provided the values of the mean effective mass m^* and high-frequency dielectric function ε_∞ are know. These values have been taken from the literature.[35] The pressure dependence of the splitting $\omega_{LO}-\omega_{TO}$ has been measured on the undoped sample *D*, and is not significantly affected by the temperature. Therefore, the value of ω_{LO} can be deduced from that of ω_{TO}, and then one can determine the variation of n_c as a function of $1/T$, for two values of the laser intensity I_0 and $I_0/20$, and depict it as an Arrhenius plot (see Figs. 4, 5, and 6). It is worthwhile to note that, below 200 K and for the three impurities, the carrier concentration presents a typical thermoactivated behavior with almost no difference as the laser power intensity is varied. For higher temperatures, the effect of the laser power intensity is important and depends on the impurity species. Here two different regimes can be distinguished in the high-temperature region.

(i) A low-pressure behavior, showing a sudden decrease of the free-carrier concentration n_c between 200 and 260 K, appears when samples are illuminated with the low power intensity $I_0/20$. Then, as the temperature increases, a thermoactivated dependence appears which presents a larger slope than that observed at low temperature. This behavior is seen in the three type of samples, but only at low pressures in GaAs:Si and GaAs:Te.

(ii) A high-pressure regime, observable only in GaAs:Si and GaAs:Te, where the effect of power density is low, and where, with increasing temperature, the thermoactivated dependence is reached without any decrease of n_c around 200 K. A change of slope is only noticeable when going from the low-temperature thermoactivated dependence to the high-temperature one (see the two upper curves in Figs. 1, 2, 4, and 5).

The temperature variation of the free-carrier concentration observed under illumination at low pressures and at low temperatures (below ~200 K) (see Figs. 1–6), is easily explained by taking into account the following processes (see also the configuration diagram drawn Fig. 7): at the thermodynamical equilibrium in the dark, the electronic concentration is controlled by the deep *DX* state (the activation energy of which is $E_{T1}>100$ meV). This situation remains unchanged, under continuous illumination, as long as the net optical ionization of the deep *DX*

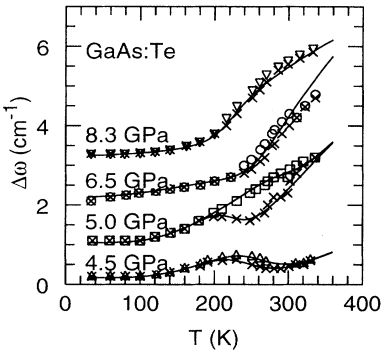

FIG. 1. Frequency splitting $\Delta\omega=\omega_+-\omega_{TO}$ vs temperature for GaAs:Te at different values of the pressure. Empty squares, triangles, and circles correspond to the laser power I_0, and crosses to $I_0/20$. Continuous curves are best fits using the negative-*U* model at 4.5 and 5.0 GPa, and the positive-*U* model at 6.5 and 8.3 GPa. (Data and curves at each pressure have been shifted along the vertical axis for clarity.)

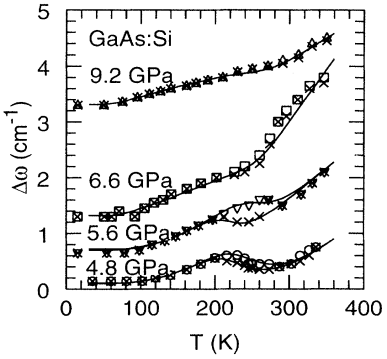

FIG. 2. Same key as in Fig. 1 but for GaAs:Si. Continuous curves are best fits using the negative-*U* model at 4.8 and 5.6 GPa, and the positive-*U* model at 6.6 and 9.2 GPa.

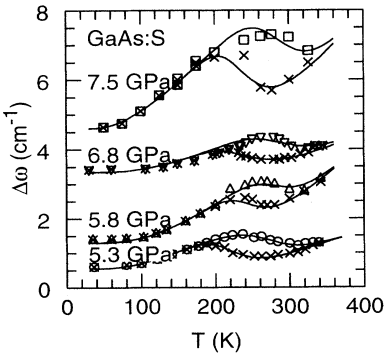

FIG. 3. Same key as in Fig. 1 but for GaAs:S. Continuous curves are best fits using the negative-*U* model at all the presented pressures.

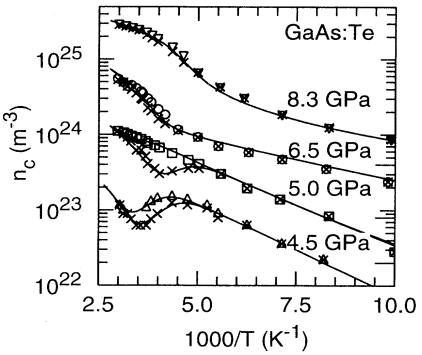

FIG. 4. Free-carrier concentration vs 1000/T for GaAs:Te. The same convention as that of Fig. 1 is adopted for the symbols. The continuous curves are deduced from the same models as those used for reproducing $\Delta\omega$ (Fig. 1). (Again, data and curves at each pressure have been shifted along the vertical axis for clarity.)

state is negligible with respect to the capture process of that deep state. When the optical generation of carriers from the deep *DX* state becomes dominant as compared to the thermal capture process, the deep *DX* level is depopulated, and the photoionized electrons are distributed between the conduction band and a shallow donor (SD) impurity level of effective-mass type (the SD state of the *DX* center which has an activation energy of ~ 50 meV). The free-carrier density variation with temperature is thus controlled by this hydrogenlike SD level.

The anomalies which are observed in Figs. 1, 2, and 3 and also in Figs. 4, 5, and 6 between 200 and 260 K and for low illumination can be interpreted in terms of trapping of the carriers by the deep *DX*-like level of the impurity, and are the signature of the bistable character of the *DX* center. Indeed, when the temperature increases, the capture rate of the deep state increases, while the optical excitation remains constant. We have to assume, therefore, that the impurity is able to trap electrons both on SD states of effective-mass type, and on deep states associated with a large lattice relation (*DX*-type state).[23] In such a picture (Fig. 7), these two levels are separated by an energetic barrier Δ of the same order of magnitude as

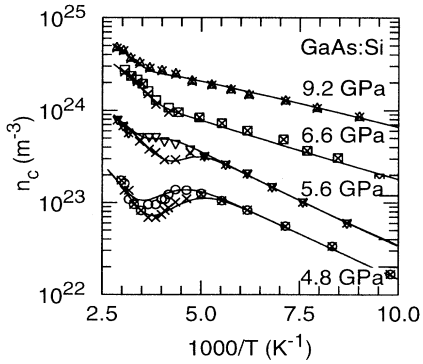

FIG. 5. Same key as in Fig. 4 but for GaAs:Si. The continuous curves are deduced from the same models as those used for reproducing $\Delta\omega$ (Fig. 2).

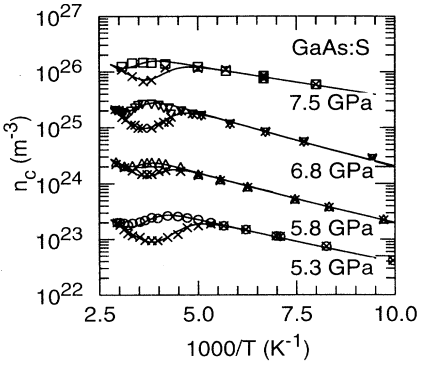

FIG. 6. Same key as in Fig. 4 but for GaAs:S. The continuous curves are deduced from the same models as those used for reproducing $\Delta\omega$ (Fig. 3).

the one E_{T1} which separates the deep *DX* level from the conduction band. This behavior is found to be the same for all impurity species, but only at low pressure for GaAs:Te and GaAs:Si samples.

At high temperatures (i.e., for $T > 260$ K) the deep state is in turn thermally ionized with an energy of about 160 ± 20 meV at ~ 7.0 GPa which increases with decreasing pressure. These values of the ionization energy of the deep state cannot be compared with results of transport measurements,[10,36–40] since these latter results have been obtained in the direct-gap configuration. There is then an interplay between SD state of effective-mass type and deep relaxed levels as visualized by the configuration diagram of Fig. 7.

The behavior of GaAs:Si and GaAs:Te at high pressures ($P > 6$ GPa) differs mainly in the low- and medium-temperature ranges ($T < 260$ K, typically) (see the upper curves of Figs. 1 and 2 and 4 and 5), where n_c is smaller compared to the low-pressure data. This means that more electrons are captured to the centers. We explain this effect by pressure-induced changes of the properties of the deep states, since it is unlikely that there are

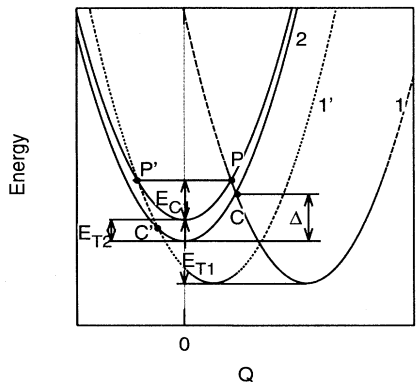

FIG. 7. Configurational diagram showing the parameters for negative- and positive-*U* models. Curve 1 and points *P* and *C* correspond to the large lattice relaxation model, and curve 1′ and points *P*′ and *C*′ are related to the small lattice relaxation case. The corresponding energy barriers are also displayed.

significant changes of the shallow states in the pressure range outside the Γ-X crossover, and moreover the observed changes do not occur in GaAs:S, i.e., they are species dependent. The relevant properties of the deep state are mainly the optical cross section, the thermal capture cross section, and the thermal emission rate for electrons. All these quantities depend on pressure, so it is difficult to say *a priori* which of them is responsible for the observed changes.

IV. RATE EQUATIONS FOR A NUMERICAL SIMULATION

In order to reproduce the experimental results (Figs. 4, 5, and 6) and to clarify the influence of the properties of the two types of *DX* center states on them, we have performed a numerical simulation of n_c based on rate equations which can be written following two different sceneries. As already mentioned, we consider two different cases which represent a negative-U model[29,30,41] [Fig. 8(a)] or a two-charge-state model (positive U) (Ref. 23) [Fig. 8(b)].

Let us first consider the negative-U model. The model supposes that three charge states are possible for the center, with respective concentrations n_1 (negatively charged), n_2 (neutral), and n_3 (positively charged). Among the transitions between these charge states, one of them, $D^- \leftrightarrow D^0$, is accompanied by a strong lattice relaxation giving rise to a barrier for the electron capture at the center. Transitions involving only one electron are considered. The excitation of the electrons from the valence band is also neglected. The rate equations can then be written as[42]

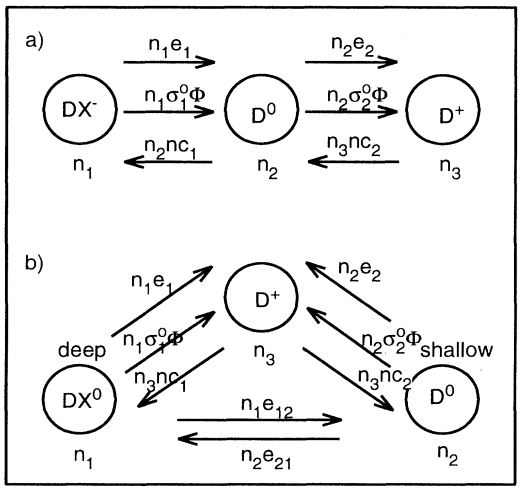

FIG. 8. Sketches of the *DX* center models used for reproducing the experimental data: (a) the negative-U model of Chadi and Chang (Ref. 29), and (b) the positive-U model proposed by Dmochowski *et al.* (Ref. 23). The circles correspond to the different energy states, and the arrows to the different transitions included in our rate equations (the transition rates are inscribed near the corresponding arrows). The two horizontal arrows (b) visualize the intracenter transitions of the two-charge-state model.

$$
\begin{aligned}
\frac{dn_1}{dt} &= -n_1e_1 - n_1\sigma_1^0\Phi + n_2n_Cc_1 \ , \\
\frac{dn_2}{dt} &= -n_2e_2 - n_2\sigma_2^0\Phi - n_2n_Cc_1 + n_1e_1 \\
&\quad + n_1\sigma_1^0\Phi + n_3n_Cc_2 \ , \\
\frac{dn_3}{dt} &= -n_3n_Cc_2 + n_2e_2 + n_2\sigma_2^0\Phi \ ,
\end{aligned}
\tag{1}
$$

where e_1, e_2, c_1, and c_2 are emission and capture rates (see the Appendix for their definition), σ_1^0 and σ_2^0 are optical cross sections for the optical ionization of an electron from D^- and D^0 states, respectively, Φ is the photon flux, and n_C is the free-electron concentration. Two additional conditions can be written for the total number of centers N_D: (i) $N_D = n_1 + n_2 + n_3$ and (ii) $N_D = 2n_1 + n_2 + n_c$. From these two equations we immediately obtain the relation $n_1 + n_c = n_3$. The details of the calculation are reported in the Appendix.

In the second model [Fig. 8(b)] we assume the existence of only two charge states (D^0 and D^+), but two different energy states correspond to the D^0 charge state—one deep and one shallow state with respective concentrations n_1 and n_2. The concentration of the positively charged state is noted n_3. We suppose that the capture of the second electron at the center is prohibited because of the positive value of the correlation energy U. The model can be then called a positive-U model with two configuration states.

The free electron can be captured at an ionized center D^+ forming either a deep state or a shallow state. We suppose that the capture process to the deep state is accompanied by the lattice distortion giving the capture barrier. The capture process by the shallow state does not exhibit any lattice distortion. Since we have two different configurations of the same center having the same charge state, we can expect direct transitions between them. In other words, due to thermal vibrations of the lattice, a center in a deep state (which is probably accompanied by certain lattice distortion) can be converted to the center in the shallow state configuration, or vice versa, without changing its charge state and *therefore involving no transport for free electrons.* These intracenter transitions imply a change of the total energy of the center, and a change of its configuration (distortion) without changing its electrical charge. The intracenter transitions can be induced by thermal or optical excitation, as this is well known for $EL2$ defect in GaAs. In our model we only include thermally driven intracenter transitions

$$
\begin{aligned}
\frac{dn_1}{dt} &= -n_1e_1 - n_1\sigma_1^0\Phi + n_Cn_3c_1 + n_2e_{21} - n_1e_{12} \ , \\
\frac{dn_2}{dt} &= -n_2e_2 - n_2\sigma_2^0\Phi + n_Cn_3c_2 + n_1e_{12} - n_2e_{21} \ , \\
\frac{dn_3}{dt} &= -\frac{dn_1}{dt} - \frac{dn_2}{dt} \ .
\end{aligned}
\tag{2}
$$

Additionally, the conservation of the total number of

centers N_D implies, $N_D=n_1+n_2+n_3$ and the condition for the total number of electrons $N_D=n_1+n_2+n_c$. From these two conditions one deduces $n_c=n_3$. Again, the details of the calculation are given in the Appendix.

Using the above equations and the formula given in the Appendix, we have been able to reproduce our experimental results with a very good agreement, over a large range of pressure and temperature (see the solid curves of Figs. 1–6). Only a reasonable number of parameters (actually five, as can be seen in Table I) have been used in order to perform the numerical simulation. The comparison with experimental data is presented in Sec. V.

V. COMPARISON WITH EXPERIMENTAL DATA AND DISCUSSION

It is useful to look at the general behavior of the calculated curves for both models. Figure 9(a) shows data taken for GaAs:S at ~ 5.3 GPa and curves calculated for the darkness and different illumination intensities. In the darkness we have a simple exponential behavior which gives the position of the deeper state. It is important to note here that the value of the activation energy of the deep state E_{T1} for the negative-U model must be $\frac{1}{2}$ of the corresponding value for the positive-U model in order to obtain the same slope of the high-temperature part of the curve. It is frequently said that negative-U statistics behaves like positive-U statistics with a high compensation ratio.[43] At high temperatures the curve bends slightly, and for $T\rightarrow\infty$ the free-electron concentration would be equal to the total number of centers N_D. When the light is on, one can observe features at low temperatures which arise due to the emptying of all deep states by light. Again, from the Arrhenius plot one can determine the position of the shallow level. In the intermediate temperature range the free-electron concentration first drops due to the increased capture rate of the deep state and then increases again due to the thermal emission rate from deep state. The position of this threshold moves to higher temperatures when increasing E_{C1}, σ_1^0, or Φ. Briefly speaking, regardless of the model the slopes are given by the positions of the shallow and deep levels in the gap. By varying N_D we can move the whole curves up or down, and by changing ΔS_1, which is the change of the entropy due to the emission of the electron [see Eq. (A3) of the Appendix], it is possible to raise or lower the high-temperature part separately. The values of E_{C1}, σ_1^0, and Φ determine the temperature range where the transition from one slope to the second one occurs. Figure 9(b) shows the comparison of the experimental data obtained for GaAs:Si at 6.6 GPa (high-pressure behavior) with the curves calculated from the positive-U (curves 1 and 2), and negative-U (curve 3) models. All parameters have the same values, with the exception of E_{T1} which is doubled for curves 1 and 2 with the respect to that of curve 3. The effect of the intracenter transitions is clearly visi-

TABLE I. List of the parameters used for reproducing the experimental data. The meaning of the symbols is explained in the text (see Sec. IV, the Appendix, and Fig. 7). The superscript $-$ at E_{T1} indicates the use of the negative-U model, whereas $+$ means the use of the positive-U model.

Impurity	Pressure GPa	E_{T1} eV	E_{C1} eV	E_{T2} eV	ΔS_1 meV/K	N_D m^{-3}	Φ $m^{-2}s^{-1}$	A s^{-1}	Δ eV
S	5.3	0.14^-	0.25	0.05	0.1	1.5×10^{24}	$1.6\times10^{27}/8\times10^{25}$		
	5.8	0.13^-	0.26	0.06	0.2	"	$8\times10^{27}/8\times10^{26}$		
	6.8	0.12^-	0.24	0.06	0.1	"	$4\times10^{27}/2\times10^{26}$		
	7.1	0.12^-	0.24	0.05	0.2	"	$3\times10^{26}/2\times10^{26}$		
	7.5	0.12^-	0.25	0.04	0.2	"	$8\times10^{27}/4\times10^{26}$		
Te	4.2	0.20^-	0.21	0.085	0.3	1.3×10^{24}	$1.2\times10^{27}/3\times10^{26}$		
	4.5	0.18^-	0.20	0.09	0.2	"	$1.5\times10^{27}/3\times10^{26}$		
	4.9	0.17^-	0.20	0.08	0.4	"	$1\times10^{27}/4\times10^{26}$		
	5.0	0.17^-	0.20	0.07	0.3	"	$1\times10^{28}/1\times10^{26}$		
	5.4	0.16^-	0.20	0.06	0.4	"	$4\times10^{27}/4\times10^{26}$		
	6.5	0.16^+	0.20	0.05	0.3	"	1×10^{26}	2×10^{7}	0.025
	7.0	0.15^+	0.20	0.05	0.3	"	2×10^{26}	2×10^{7}	0.03
	8.3	0.12^+	0.20	0.05	0.3	"	1×10^{26}	3×10^{7}	0.035
Si	4.3	0.19^-	0.23	0.06	0.2	1.5×10^{24}	1×10^{26}		
	4.8	0.17^-	0.24	0.07	0.2	"	$8\times10^{26}/2\times10^{26}$		
	5.1	0.17^-	0.23	0.07	0.3	"	$6\times10^{27}/3\times10^{26}$		
	5.3	0.16^-	0.22	0.06	0.4	"	$1\times10^{28}/1\times10^{26}$		
	5.6	0.15^-	0.24	0.065	0.4	"	$6\times10^{27}/3\times10^{26}$		
	5.7	0.15^-	0.24	0.065	0.4	"	$6\times10^{27}/3\times10^{26}$		
	6.3	0.16^+	0.22	0.06	0.3	"	6×10^{26}	1×10^{7}	0.025
	6.6	0.15^+	0.22	0.05	0.3	"	2×10^{26}	1×10^{7}	0.025
	6.7	0.15^+	0.22	0.05	0.3	"	2×10^{26}	2×10^{7}	0.03
	8.1	0.12^+	0.23	0.05	0.3	"	1×10^{26}	2×10^{7}	0.03
	9.2	0.12^+	0.23	0.04	0.3	"	1×10^{26}	1×10^{7}	0.035

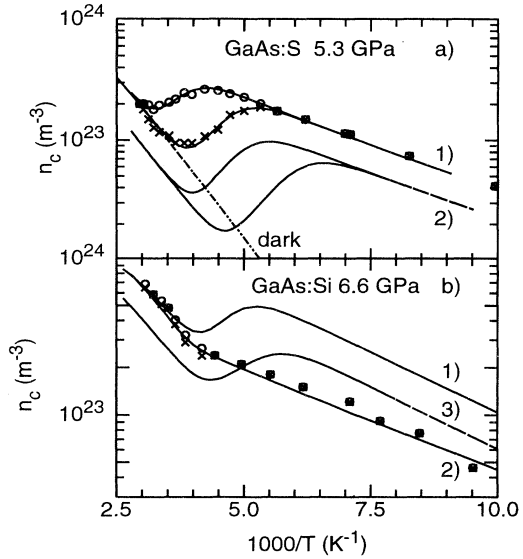

FIG. 9. (a) Arrhenius plot showing the experimental data obtained for GaAs:S at 5.3 GPa, and the calculated curves using the positive-U (1) and negative-U (2) models. Empty circles correspond to the laser power I_0, and crosses to $I_0/20$. The calculations reproduce the effect of the illumination intensity. The calculated curve for darkness is also plotted. All parameters of the curves are identical, with the exception of the activation energy of the deep state E_{T1} for the negative-U model. (b) Comparison of the experimental data obtained for GaAs:Si at 6.6 GPa with the calculated curves obtained using the positive-U model without [curve (1)] or with [curve (2)] intracenter transitions, and the negative-U model [curve (3)]. Again, the empty circles correspond to the laser power I_0, and crossed to $I_0/20$, and all the parameters are the same with the exception of E_{T1}.

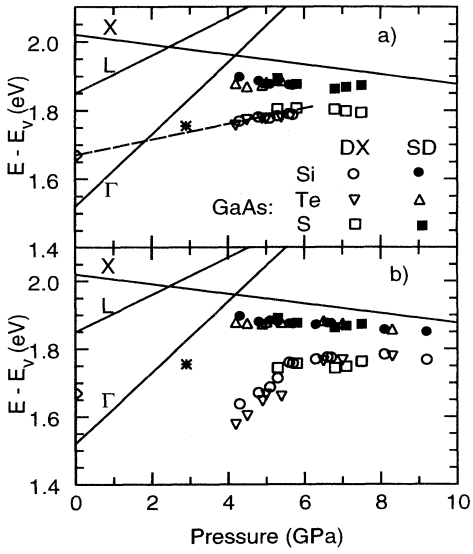

FIG. 10. Energy position of the SD and deep levels for the negative-U (a) and positive-U (b) models. Points at 1 bar and 2.9 GPa are those given in Refs. 7 and 11, respectively. The dashed line in (a) corresponds to a slope of 22 meV/GPa.

ble: they are switched off for curve 1 and on for curve 2, and they appear to be essential in order to reproduce the experimental data at high pressure. The intracenter transitions included in the two-charge-state model mainly influence the low-temperature part of the curves, moving them down (with respect to the high-temperature part) and changing their slopes slightly. Results of our fitting analysis are given in Table I and illustrated in Fig. 10.

Both models well fit our experimental data obtained with GaAs:S, and also with GaAs:Si and GaAs:Te, but only for the low-pressure range (see Figs. 1–6). Indeed, only the positive-U model, due to the possibility of intracenter transitions, is able to describe the high-pressure behavior observed for GaAs:Si and GaAs:Te. One can observe that the activation energy of the SD level (energy E_{T2} in Table I and Fig. 7) does not depend on the impurity species. It unambiguously follows the X minimum behavior with pressure in the indirect-gap regime, whereas the deep-state energy position E_{T1} is rather less sensitive to pressure in the same pressure range. The value of this E_{T2} energy is found to be about 50 ± 10 meV at high pressures, and deepens slightly when the pressure decreases. This has to be compared to the binding energy of the effective-mass-like level, which is about 66 meV, as found for GaP:Te, for example, at this high level of doping.[44] These features for E_{T2} are given by long-range and slowly varying Coulombic tails of the defect potential. Both models we use treat the shallow state in the same way (one-electron state, no capture barrier), so that both models lead to the same values of the SD energy position in the gap. This is not the case of the deep *DX* level, for which different energies E_{T1} are obtained when using different models (see Table I and Fig. 10). The activation energies E_{T1} of deep state for silicon and tellurium impurities, determined for the positive-U model, reveal a sharp change around 5 GPa [see Fig. 10(b)], which is not expected for a pressure variation of a deep level. Furthermore, these values of activation energy do not fit previous results obtained at low pressure[7,11] [Fig. 10(b)]. The easiest way to explain these anomalies is to assume that the positive-U model is not appropriate below that pressure. Therefore, the shape of the curves observed at low pressures is characteristic of the negative-U models, which turns out to be valid for the S impurity up to the highest pressure. Including previous data,[7,11] we obtain a pressure dependence of the deep *DX* negative-U level of 22 ± 2 meV/GPa [see Fig. 10(a)]. On the other hand, it is natural to associate the change in the shape of the curves with the change of the sign of the energy U for the other impurities, a change occurring in the range 5–6 GPa. Such a change of the sign of the Hubbard correlation energy U has already been predicted by Baj, Dmowski, and Slupinski.[32] The parameters used for fitting can be compared with some existing values reported in the literature, as for instance E_{C1} for $Al_xGa_{1-x}As$:Si:[40] the agreement is quite good. The parameters A and Δ describing the rate of the intracenter transitions are displayed in Table I for tellurium and silicon for high pressures only, because for lower pressures their relative contribution was not important.

In the positive-U model, the two paths of the reversible transition from deep to shallow states are present. The

probability of both processes is mainly governed by the height of the corresponding barriers (E_{C1},Δ). At high pressure the intracenter transitions prevail, with a small barrier Δ with respect to E_{C1}: this is only compatible with the small lattice relaxation picture. However, at lower pressures the transitions via the conduction band are more important when the negative-U model is effective with a large lattice relaxation.[28–30,45] This can be explained by a pressure-induced change of the equilibrium lattice coordinate Q_0. The transition from the negative- to positive-U model should occur with a change in the lattice relaxation.

The negative-U model proposed by Chadi and coworkers[29,30,45] is compatible with our data at lower pressures with a stable configuration made of a negatively charged two-electron state with a broken-bond configuration. The impurity atom is displaced in the $\langle 111 \rangle$ direction. When increasing the pressure the interatomic distances decrease, so that the impurity atom is forced to return to its lattice position; in other words, the symmetrically distorted neutral state becomes energetically more favorable. This state reveals a small symmetrical lattice relaxation, giving a still-high capture barrier but a much smaller barrier for intracenter transitions so that this channel remains efficient. Schematically this is sketched in Fig. 7. The sulfur impurity for all pressures between 5.3 and 7.5 GPa behaves as a negative-U impurity. This exception could be explained by comparing the tetrahedral covalent radii of impurities with a nearest-neighbor distance[46] in the GaAs lattice (=2.45 Å). The atomic radius of a silicon atom is 1.17 Å, and 1.32 Å, for tellurium, but only 1.04 Å for sulfur,[46] so that the sulfur atoms could remain in the broken-bond configuration even at high pressures. The pressure of 5.5 GPa causes the decrease of the lattice constant of GaAs by 0.05 Å (according to the Murnaghan equation[47]) which is not much but is still six times more than the difference between the lattice constant of GaAs and AlAs.[48] Note also that the pressure of 17 GPa is able to transform completely the crystal lattice of GaAs. It appears that the pressure effect is much stronger than the alloying effect, and this could explain why such a transition between the negative- and positive-U models in $Al_xGa_{1-x}As$ alloys has never been observed.

The existence of the crossover between the two models is also supported by the different pressure dependences of the energies (Fig. 10). For a very deep state, the level does not follow any minimum of the conduction band, which means that its wave function consists of the Bloch functions with a $\mathbf{k}$ vector from the whole Brillouin zone. Chadi and Chang[29] approximated the influence of the conduction-band minima according to their multiplicity and their formula for the pressure dependence of the deep state (with respect the valence band) reads

$$\frac{dE_{T1}}{dp}=\frac{1}{8}\left[\frac{dE_\Gamma}{dp}+3\frac{dE_X}{dp}+4\frac{dE_L}{dp}\right]=+36\,\text{meV/GPa}\ . \tag{3}$$

This formula overestimates the expected pressure coefficient since it does not stress the differences in the density of states between the three minima of the conduction band. For that reason this compares quite well with our results (22±2 meV/GPa) at low pressures with the negative-U model [Fig. 10(a)]. On the other hand, a positive-U model with a small lattice relaxation looks very much like an effective-mass-type center, and it is not surprising that at high pressures this level follows the X-band minima quite well [Fig. 10(b)].

VI. CONCLUSION

In conclusion, the study of GaAs samples doped with Si, Te, and S, as a function of hydrostatic pressure and of temperature, reveal the bistability of the related impurity level under optical illumination. This bistability involves a shallow effective-mass-like level and a deep level. The character of this deep level is not unique. It is possible to describe the behavior of the sulfur impurity with a negative-U model for the pressure range up to 7.5 GPa, whereas for Te and Si impurities a crossover behavior from negative to positive U occurs in the range 5–6 GPa. This is accompanied by a transition from a LLR to a SLR state.

Thus we can conclude from our results that the DX center is a defect which evolves with pressure, and that a single model is not able to reproduce the experimental data over a large pressure range.

ACKNOWLEDGMENTS

One of us (J.Z.) acknowledges support from Grant No. 202/93/1160 of the Czech Grant Agency. The High Magnetic Field Laboratory is Laboratoire Associé à l'Université Joseph Fourier-Grenoble.

APPENDIX: DX CENTER STATISTICS

Here we present the equations and the hypothesis which we used in our numerical simulation. The system of equations (1) and (2) (see Sec. IV) provides solutions in the steady-state case. In the case of system (1), the steady-state solution is given by the cubic equation for n_C:

$$n_c^3 a_1 a_2 + n_c^2 a_2 (N_D a_1 + 1) + n_C - N_D = 0\ , \tag{A1}$$

where

$$a_1=\frac{c_1}{e_1+\sigma_1^0\Phi}\ ,\quad a_2=\frac{c_2}{e_2+\sigma_2^0\Phi}\ . \tag{A2}$$

The relations for the capture rates and for the emission rates are

$$e_1=\sigma_1^\infty \bar{v} N_C g_1^{-1} \exp\left[-\frac{E_{T1}+E_{C1}-T\Delta S_1}{kT}\right]\ ,$$
$$c_1=\sigma_1^\infty \bar{v} \exp\left[-\frac{E_{C1}}{kT}\right]\ , \tag{A3}$$

$$e_2=\sigma_2^{\infty}\bar{v}N_C g_2^{-1}\exp\left[-\frac{E_{T2}+E_{C2}}{kT}\right],$$
$$c_2=\sigma_2^{\infty}\bar{v}\exp\left[-\frac{E_{C2}}{kT}\right], \tag{A4}$$

where σ_1^{∞} and σ_2^{∞} are capture cross-section prefactors, $\bar{v}$ is the mean velocity of electrons, N_C is the effective density of states of the conduction band (related to the X minimum in our case), g_1 and g_2 are degeneracy factors, E_{T1} and E_{T2} are the thermal activation energies which give the position of the energy levels in the gap, and E_{C1} and E_{C2} are the capture barriers. For the $D^0 \leftrightarrow D^+$ transitions, the change of entropy of the shallow state ΔS_2 due to the emission of the electron is supposed to be zero because of the effective-mass nature of this state. For the same reason we assume $E_{C2}=0$.

In the case of the positive-U model [Fig. 8(b)], the steady-state solution of the system of equations (2) is given by a quadratic equation

$$n_C^2(a_1+a_2)+n_C-N_D=0\ , \tag{A5}$$

where a_1 and a_2 are now given by

$$a_1=\frac{c_1+\dfrac{c_2e_{21}}{e_2+e_{21}+\sigma_2^0\Phi}}{e_1+\sigma_1^0\Phi+e_{12}-\dfrac{e_{12}e_{21}}{e_2+e_{21}+\sigma_2^0\Phi}},$$
$$a_2=\frac{c_2+\dfrac{c_1e_{12}}{e_{12}+e_1+\sigma_1^0\Phi}}{e_2+\sigma_2^0\Phi+e_{21}-\dfrac{e_{21}e_{12}}{e_1+e_{12}+\sigma_1^0\Phi}}. \tag{A6}$$

One can see that Eq. (A5) is perfectly symmetrical with respect to the coefficients a_1 and a_2, which is quite natural and clearly visible from Fig. 8(b). The emission and capture rates for both states are expressed again by (A3) and (A4). In order to estimate the rates e_{12} and e_{21}, one can look at the configuration coordinate diagram displayed in Fig. 7. The crossing point P is important for thermally activated transitions of an electron from the deep state (1) to the conduction band and back. The crossing point C at the intersection of parabolas 1 and 2 is relevant for the intracenter transition from the deep-state configuration to the shallow one or back without changing the charge state of the center. If we denote Δ the thermal energy barrier necessary for the transition from the shallow state to the deep one, then the barrier for the reverse process is $\Delta+E_{T1}-E_{T2}$, and then

$$e_{21}=A\exp\left[-\frac{\Delta}{kT}\right],$$
$$e_{12}=A\exp\left[-\frac{\Delta+E_{T1}-E_{T2}}{kT}\right], \tag{A7}$$

where A is a prefactor which has to be fitted. If we assume that the curvature of all three parabolas in Fig. 7 is the same, then the barrier height Δ can be expressed as a function of the other barrier energies in the following way:

$$\Delta=\frac{E_{C1}+E_{T1}}{2}-\frac{E_{T1}}{4}\pm\frac{\sqrt{E_{C1}(E_{C1}+E_{T1})}}{2}$$
$$+\frac{(E_{T2}-E_{T1})^2}{8E_{C1}+4E_{T1}\pm\sqrt{E_{C1}(E_{C1}+E_{T1})}}\ . \tag{A8}$$

Equation (A8) has two solutions because for given values of E_{T1} and E_{C1} there exist two different configurational coordinate diagrams: one corresponding to a small lattice relaxation (see curve 1′ in Fig. 7), a second one exhibiting a large lattice relaxation (curve 1 in Fig. 7).[49] One can see that for given values of E_{C1}, E_{T1}, and E_{T2}, the heights of the corresponding barrier Δ differ significantly.

From the above expressions it is clear that there are many parameters included in the models. In our fitting procedure we have tried to keep fixed as many parameters as possible, and to follow the pressure dependences of the remaining ones. The coefficients a_1 and a_2 contain parameters describing the properties of the host semiconductor and the *DX* center. The host material is characterized by the effective mass of electrons m^*, the effective density of states N_c, and the mean velocity of the electrons in the conduction band $\bar{v}$. The effective density of states and the mean velocity $\bar{v}$ have been calculated using the standard formula

$$N_c=2s\left[\frac{2\pi m^*kT}{h^2}\right]^{3/2},\quad \bar{v}=\left[\frac{3kT}{m^*}\right]^{1/2}, \tag{A9}$$

where s is the multiplicity of the X minima (here $s=3$), and h is Planck's constant. The following parameters were kept unchanged for fitting all curves: $\sigma_1^{\infty}=1\times10^{-18}$ m^2,[40] and $\sigma_1^0=\sigma_2^0=1\times10^{-21}$ m^2.[43,50,51] The solutions for both models are almost insensitive to the values of σ_2^{∞} and σ_2^0 as long as thermal emission rate e_2 is much larger than the optical emission rate $\sigma_2^0\Phi$, because then $a_2 \propto c_2/e_2=g_2/N_c\exp(-E_{T2}/kT)$. Thus in a first approximation we have taken $\sigma_2^{\infty}=\sigma_1^{\infty}$ and $\sigma_2^0=\sigma_1^0$. The energies E_{C1}, E_{T1}, and E_{T2} depend on the hydrostatic pressure and have to be fitted. The degeneracy factors have been taken as $g_1=g_2=2$. Finally, only five parameters were adjusted in order to perform our numerical simulation (see Table I). Using the above values and taking the appropriate slopes from our experimental curves as first approximations of the values E_{T1} and E_{T2}, we obtained a fairly good agreement between calculated and measured curves (see Figs. 1–6).

[1]*Physics of DX Centers in GaAs Alloys,* edited by J. C. Bourgoin, Solid State Phenomena Vol. 10 (Sci-Tech, Brookfield, VT, 1990).

[2]Proceedings of the Symposium on DX Centers and other Metastable Defects in Semiconductors [Semicond. Sci. Technol. **6**, 10B (1991)].

[3]P. M. Mooney, J. Appl. Phys. **67**, R1 ((1990).

[4]*DX Centers-Donors in AlGaAs and Related Compounds,* edited by E. Muñoz Merino, Defect and Diffusion Forum Vol. 108 (Scitec, Zug, Switzerland, 1994).

[5]A. K. Saxena, Appl. Phys. Lett. **36**, 79 (1980).

[6]M. Mizuta, M. Tachikawa, H. Kukimoto, and S. Minomura, Jpn. J. Appl. Phys. **24**, L143 (1985).

[7]D. K. Maude, J. C. Portal, L. Dmowski, T. Foster, L. Eaves, M. Nathan, M. Heiblum, J. J. Harris, and R. B. Beall, Phys. Rev. Lett. **59**, 815 (1987).

[8]M. F. Li, W. Shan, P. Y. Yu, W. L. Hansen, E. R. Weber, and E. Bauser, Appl. Phys. Lett. **53**, 1195 (1988).

[9]M. Tachikawa, T. Fujizawa, H. Kukimoto, A. Shibata, G. Oomi, and S. Minomura, Jpn. J. Appl. Phys. **24**, L893 (1985).

[10]T. Suski, R. Piotrzkowski, P. Wisniewski, E. Litwin Staszewska, and L. Dmowski, Phys. Rev. B **40**, 4012 (1989).

[11]M. F. Li, P. Y. Yu, E. R. Weber, and W. Hansen, Phys. Rev. B **36**, 4531 (1987); Appl. Phys. Lett. **51**, 349 (1987).

[12]P. M. Mooney, E. Calleja, S. L.Wright, and M. Heiblum, in *Proceedings of the 14th International Conference on Defects in Semiconductors, Paris, France, 1986,* edited by H. J. von Bardeleben, Materials Science Forum Vol. 10 (Trans Tech, Aedermannsdorf, Switzerland, 1986), p. 417.

[13]E. Calleja, F. Garcia, A. L. Romero, E. Muñoz, A. L. Powell, P. I. Rokett, C. C. Button, and J. S. Roberts, Semicond. Sci. Technol. **7**, 758 (1992).

[14]V. Šmíd, J. Krištofik, J. Zeman, and J. J. Mareš, Semicond. Sci. Technol. **6**, B150 (1991); Philos. Mag. B **67**, 25 (1993).

[15]M. Leroux, J. M. Sallèse, J. Leymarie, G. Neu, and P. Gibart, Semicond. Sci. Technol. **6**, 514 (1991); J. Leymarie, M. Leroux, and G. Neu, Phys. Rev. B **42**, 1482 (1990).

[16]M. Zigone, P. Seguy, M. Roux-Buisson, and G. Martinez, in *Proceedings of the 15th International Conference on Defects in Semiconductors, Budapest, Hungary, 1988,* edited by G. Ferenczi, Materials Science Forum Vols. 38-41 (Trans Tech, Aedermannsdorf, Switzerland, 1989), p. 1097.

[17]J. E. Dmochowski, R. A. Stradling, P. D. Wang, S. N. Holmes, M. Li, B. D. McCombe, and B. Weinsten, Semicond. Sci. Technol. **6**, 476 (1991).

[18]P. Gibart, D. L. Williamson, J. Moser, and P. Basmaji, Phys. Rev. Lett. **65**, 1144 (1990).

[19]P. Seguy, M. Zigone, and G. Martinez, Phys. Rev. Lett. **68**, 518 (1992).

[20]J. Zeman, P. Seguy, M. Zigone, and G. Martinez, in *Proceedings of the 21st International Conference on Physics of Semiconductors, Beijing, China, 1992,* edited by Ping Jiang and Hou-Zhi-Zheng (World Scientific Singapore, 1993), p. 1549.

[21]M. Mizuta and K. Mori, Phys. Rev. B **37**, 1043 (1988).

[22]D. K. Maude, U. Willke, M. L. Fille, P. Gibart, and J. C. Portal, in *Shallow Impurities in Semiconductors,* edited by T. Taguchi, Material Science Forum Vols. 117-118 (Trans Tech, Aedermannsdorf, Switzerland, 1993), pp. 441–446; M. L. Fille, U. Willke, D. K. Maude, J. M. Sallese, M. Rabary, J. C. Portal, and P. Gibart, in *Proceedings of the International Symposium on GaAs and Related Compounds, Freiburg, 1993,* edited by H. S. Rupprecht and G. Weimann, IOP Conf. Proc. No. 136 (Institute of Physics and Physical Society, London, 1994), p. 761.

[23]J. E. Dmochowski, J. M. Langer, J. Raczynska, and W. Jantsch, Phys. Rev. B **38**, 3276 (1988); **40**, 9671 (1989).

[24]P. M. Mooney, W. Wilkening, U. Kaufmann, and T. F. Kuech, Phys. Rev. B **39**, 5554 (1989).

[25]H. J. von Bardeleben, J. C. Bourgoin, P. Basmaji, and P. Gibart, Phys. Rev. B **40**, 5892 (1989); H. J. von Bardeleben, M. Zazoui, S. Alaya, and P. Gibart, *ibid.* **42**, 1500 (1990).

[26]Y. B. Jia, M. F. Li, J. Zhou, J. L. Gao, M. Y. Kong, P. Y. Yu, and K. T. Chan, J. Appl. Phys. **66**, 5632 (1989).

[27]J. A. Wolk, W. Walukiewicz, M. L. W. Thewalt, and E. E. Haller, Phys. Rev. Lett. **68**, 3619 (1992).

[28]B. H. Cheong and K. J. Chang, Phys. Rev. Lett. **71**, 4354 (1993).

[29]D. J. Chadi and K. J. Chang, Phys. Rev. Lett. **61**, 873 (1988); Phys. Rev. B **39**, 10 063 (1989).

[30]S. B. Zhang and D. J. Chadi, Phys. Rev. B **42**, 7174 (1990).

[31]T. Fujisawa, J. Yoshino, and H. Kukimoto, Jpn. J. Appl. Phys. **29**, L388 (1990); in *Proceedings of the 20th International Conference on the Physics of Semiconductors, Thessaloniki, Greece, 1990,* edited by E. M. Anastassakis and J. D. Joannopuolos (World Scientific, Singapore, 1990), p. 509.

[32]M. Baj, L. H. Dmowski, and T. Slupinski, Phys. Rev. Lett. **71**, 3529 (1993).

[33]E. Yamaguchi, K. Shiraishi, and T. Ohno, J. Phys. Soc. Jpn. **60**, 3093 (1991).

[34]G. Abstreiter, M. Cardona, and A. Pinczuk, in *Light Scattering in Solids IV,* edited by M. Cardona and G. Guntherodt (Springer-Verlag, Berlin, 1984).

[35]*Semiconductors, Physics of Group IV Elements and III-V Compounds,* edited by O. Madelung, Landolt-Börnstein, New Series, Group III, Vol. 17, Pt. a (Springer-Verlag, Berlin, 1982).

[36]D. V. Lang, in *Deep Centers in Semiconductors,* edited by S. T. Pantelides (Gordon and Breach, New York, 1986).

[37]P. J. Antony, J. L. Zilko, V. Swaminathan, N. E. Schumaker, W. R. Wagner, and J. C. Norberg, Appl. Phys. Lett. **38**, 434 (1981).

[38]E. Calleja, E. Muñoz, A. Gomez, and B. Jimenez, J. Appl. Phys. **59**, 2335 (1986); **57**, 5295 (1985).

[39]M. Zazaoui, S. L. Feng, and J. C. Bourgoin, Phys. Rev. B **41**, 8485 (1990).

[40]E. Calleja and E. Muñoz, in *Physics of the DX Centers in GaAs Alloys,* edited by J. C. Bourgoin, Solid State Phenomena Vol. 10 (Sci-Tech, Liechtenstein, 1990).

[41]J. M. Langer, J. E. Dmochowski, L. Dobaczewski, W. Jantsch, and G. Brunthalter, in *Physics of DX Centers in GaAs Alloys* (Ref. 40).

[42]J. S. Blakemore, *Semiconductor Statistics* (Pergamon, Oxford, 1962).

[43]L. Dobaczewski and J. M. Langer, in *Shallow Impurities in Semiconductors,* edited by G. Davies (Trans Tech, Aedermannsdorf, 1991), p. 433.

[44]H. C. Montgomery, J. Appl. Phys. **39**, 2002 (1968).

[45]D. J. Chadi, Phys. Rev. B **46**, 6777 (1992).

[46]L. Pauling, in *The Nature of the Chemical Bond,* 3rd ed. (Cornell University Press, Ithaca, NY, 1960), p. 246.

[47]F. D. Murnaghan, Proc. Natl. Acad. Sci. **30**, 244 (1944).

[48]M. Neuberger, *III-V Ternary Semiconducting Compounds, Data Tables, IFI* (Plenum, New York, 1972), p. 8.

[49]M. F. Li and P. Y. Yu, Solid State Commun. **61**, 13 (1987).

[50]D. V. Lang, R. A. Logan, and R. Jaros, Phys. Rev. B **19**, 1015 (1979).

[51]P. A. Mooney, G. A. Northtrop, T. N. Morgan, and H. G. Grimmeiss, Phys. Rev. B **37**, 8298 (1988).